J Solution Chem (2010) 39: 1061–1086
DOI 10.1007/s10953-010-9559-0

Spectral Characteristics of Sulfa Drugs: Effect of Solvents, pH and β-Cyclodextrin

A. Antony Muthu Prabhu · G. Venkatesh · N. Rajendiran

Received: 12 December 2009 / Accepted: 19 February 2010 / Published online: 14 July 2010

Abstract The absorption and fluorescence spectra of sulfamethoxazole (SMO), sulfisoxazole (SFO), sulfathiazole (STO) and sulfanilamide (SAM) in different solvents, pH and β-cyclodextrin (β-CD) have been analyzed. The inclusion complexes of the above sulfa drugs with β-CD were investigated by UV-visible spectroscopy, fluorometry, DFT, SEM, FT-IR and ^{1}H NMR. The solvent study indicates that the position of the substituent (oxazole or thiazole group) in the SAM molecule (R–SO_2–NH-group) is not the key factor to change the absorption and emission behavior of these sulpha drug molecules. In aqueous solution, a single fluorescence band (340 nm) was observed whereas in solutions of β-CD dual emission (430 nm) was noticed in sulpha drug compounds. Formation of the inclusion complex in SMO, SFO and STO should result dual emission which is due to a Twisted Intramolecular Charge Transfer band (TICT). The β-CD study indicates that (i) sulpha drugs form 1:1 inclusion complexes with β-CD and (ii) the red shift and the presence of TICT in the β-CD medium confirms heterocyclic ring encapsulated in the β-CD cavity with the aniline ring present on the out side of the β-CD cavity.

Keywords Sulfa drugs · Solvent effects · β-Cyclodextrin · TICT · Inclusion complex

1 Introduction

In recent years, molecules of β-cyclodextrin (β-CD) have been shown to be interesting micro vessels for several molecules and the resulting supramolecular species serve as excellent miniature models for enzyme substrate complexes [1–3]. The reduced polarity and the restricted space provided by the β-CD cavity markedly influence a number of photo physical properties of the drug molecules. In addition, especially in pharmaceutical industries, the inclusion process of drug molecules in β-CDs leads to important modifications of pharmaceutical properties of drug molecules. For example, the pharmaceutical interest in β-CDs extends to enhanced solubility, chemical stability and bioavailability of poorly soluble

A.A. Muthu Prabhu · G. Venkatesh · N. Rajendiran (✉)
Department of Chemistry, Annamalai University, Annamalai nagar 608 002, Tamilnadu, India
e-mail: drrajendiran@rediffmail.com

drugs, to reduced toxicity and to control of the rate of release. The size of the β-CD and the drug molecule plays an important role to determine the complex type or stoichiometry.

Further, it is known that cyclodextrins (CD) have the property of forming inclusion complexes with guest molecules that have suitable characteristics of polarity and dimension [1–3]. The inclusion complex formation in the CD systems is favored by substitution of the high-enthalpy water molecules located inside the CD cavity, with an appropriate guest molecule of low polarity. An overview of the non-chromatographic analytical uses of CDs has been presented by Szejtli [3]. As the complexation process implies an interaction producing a protection of the included species, the CDs have been used in the pharmaceutical industry to encapsulate drugs that are photosensitive. There are a few reports dealing with the analytical determination of sulphonamides by using CD and they employ, in general, a capillary electrophoresis technique. In the case of SMO, Okamoto et al. [4] used dimethyl-β-cyclodextrin as a modifier of the mobile phase in micellar electro-kinetic chromatography and β-CD is used in capillary electrophoresis. Muñoz de la Peña et al. [5] made fluorescence measurements in pharmaceutical preparations of the inclusion complex of SMO in β-CD.

Among the many and different families of organic inorganic chemicals being currently investigated because of their applications, sulfonamides and their N-derivatives are one of the outstanding groups. Sulfonamides were the first effective chemotherapeutic agents employed systematically for the prevention and cure of bacterial infections in humans. After the introduction of penicillin and other antibiotics, the popularity of sulfonamides decreased. However, they are still considered useful in certain therapeutic fields, especially in the case of ophthalmic infections as well as infections in the urinary and gastrointestinal tract. Besides, sulfa drugs are still today among the drugs of first election (together with ampicillin and gentamycin) as chemotherapeutic agents in bacterial infections by Escherichia coli in humans. The sulfanilamides exert their antibacterial action by the competitive inhibition of the enzyme dihydropterase synthetase towards the substrate p-aminobenzoate.

Sulphonamides belong to the group of antibacterial drugs which are used for human and animal therapy, to cure infectious diseases of digestive and respiratory systems, infections of the skin (in the form of ointments) and for prevention or therapy of coccidiosis of small domestic animals [6]. Quality control of sulphonamide formulations and their quick systematic monitoring in body fluids are important analytical tasks. A number of articles have been published concerning the determination of sulphonamides by different analytical methods.

Sulphamethoxazole (SMO) is widely used as an antibacterial, mainly in combination with trimethroprim. This is a well-recognized preparation, as the combination of a sulphonamide with an inhibitor of the dihydropholate reductase increases the bacteriostatic effect of the sulphonamide, by blocking the metabolic pathways of the microorganisms at two different points. Different methods have been described for determining the sulphonamides, but, in general, they are based on separation methods using different detection types. Its determination in urine has been made by micellar liquid chromatography and by supported liquid membrane with high pressure liquid chromatography-electrospray mass spectrometry detection [7].

The fluorescence characteristics of different sulphonamides have been studied [8] and proposed for the determination of several of these compounds. Thus, sulphanilamide can be determined by reaction with homophthaldehyde. The analysis of sulphadrugs [9, 10] has been performed in foods and pharmaceuticals using the fluorescamine reaction. The reaction of 9-cloroacridine with sulphonamides produces a fluorescence quenching which allows the determination of sulphonamides [11]. Sulpha drugs were determined in milk and pharmaceutical preparations by photochemically-induced fluorometry [12]. Fluorescence has also

been used as HPLC detection for determining sulpha drugs in milk and eggs [13] and recently, fluorescence after pre-column derivatization with fluorescamine has been applied as a detection technique [13].

In this work, we not only studied spectral properties of sulpha drug–β-CD complexes by UV-visible and fluorescence, but also prepared their solid inclusion complexes by the co-precipitation method and determined their formation by FT-IR, ^{1}H NMR, SEM and DFT methods. The formation constant of the inclusion complex were obtained according to UV-visible and fluorescence data using the modified Benesi-Hildebrand equation. The solid studies on the inclusion complex of β-CD with guest molecules have been performed to obtain direct evidence for the formation of the inclusion complexes. The obtained results indicate that the solid structure of these complexes is designable by appropriately selecting of the type, length and functional substituent group in the guest.

2 Materials and Methods

2.1 Instruments

Absorption spectral measurements were carried out with a Hitachi Model U-2010 UV-visible spectrophotometer and fluorescence measurements were made using a Shimadzu RF 5301 spectrofluorimeter. In both instruments for measurement of the readings we used a quartz cell and the width of this cell is 1 cm and the height is 4.5 cm. We used the excitation wavelength 270 nm for all the sulpha drugs. The pH values in the range 2.0–12.0 were measured on Elico pH meter model LI-120. FT-IR spectra were obtained with Avatar-330 FTIR spectroscopy using KBr pelleting. The range of spectra was from 500 to 4000 cm^{-1}. Microscopic morphological structure measurements were performed with a JEOL JSM 5610 LV scanning electron microscope (SEM).

2.2 Reagents and Materials

SMO, SFO, STO, SAM, β-CD and all the spectrograde solvents were obtained from the Sigma-Aldrich chemical company and used as such. The purity of the compound was checked by similar fluorescence spectra when excited with different wavelengths. Triply distilled water was used for the preparation of aqueous solutions. Solutions in the pH range 2.0–12.0 were prepared by adding appropriate amounts of NaOH and H_3PO_4. A modified Hammett's acidity scale (H_0) [14] for the solutions below pH $\sim$2 (using a H_2SO_4–H_2O mixture) and Yagil's basicity scale (H) [15] for solutions above pH$\sim$12 (using a NaOH–H_2O mixture) were employed. The solutions were prepared just before taking measurements. The concentration of the sulfa drug solutions was of the order 2×10^{-4} to 2×10^{-5} Mol·L^{-1}. The concentration of the β-CD solution was varied from 1×10^{-3} to 1×10^{-2} Mol·L^{-1}.

2.3 Preparation of Solid Complex of Sulfa Drugs with β-CD

Accurately weighed β-CD (1.2 g) was taken in a 50 mL conical flask and dissolved in 30 mL distilled water. Then, sulpha drugs were taken in a 50 mL beaker and 20 mL distilled water was added and stirred on an electromagnetic stirrer until it was dissolved. The β-CD solution was slowly poured into the sulpha drugs solution. This mixed solution was continuously stirred for 48 hrs at 50 °C. The reaction mixture was refrigerated for 48 hrs. White crystal were precipitated, which were filtered with a G_4 sand filter funnel and washed with distilled water. After drying in an oven at 60 °C for 12 hrs a white powder product was obtained, which was the inclusion complex of the sulpha drug with β-CD.

3 Results and Discussion

3.1 Effect of Solvents

Table 1 depicts the absorption maxima, $\log_{10}\varepsilon$ and fluorescence maxima of sulfisoxazole (SFO, N^1-(3,4-dimethyl-5-isoxazolyl) sulfanilamide), sulfamethoxazole (SMO, N^1-(5-methyl-3- isoxazolyl)sulfanilamide), sulfathiazole (STO, N^1-(2-thiazolyl) sulfanilamide) and sulfanilamide (SAM, 4-aminobenzene sulfonamide) in the solvents of different polarity and hydrogen bond forming tendency as well as at different proton concentrations (Scheme 1). Because of the very low solubility of sulfa drugs in cyclohexane, their maxima were obtained using 1% dioxane solutions of cyclohexane. These maxima will be very near to the maxima obtained from pure cyclohexane as the polarity of dioxane is close to cyclohexane. Furthermore the trend observed in the maxima of sulfa drugs in cyclohexane is similar to the trend in other solvents. Data in Table 1 clearly indicate that the absorption spectra of the above molecules are red shifted from cyclohexane to methanol, but compared to methanol a blue shift is observed in water. The red shift increases according to the following sequence: SAM < SMO = STO = SFO. The above sequence indicates the position of the substituent (oxazole or thiazole group) in the SAM molecule (R–SO_2–NH)-group is not the key factor to change the absorption behavior of these molecules. When compared to aniline [16] (cyclohexane, $\lambda_{abs} \sim 283$, 235 nm, $\lambda_{flu} \sim 320$ nm, methanol, $\lambda_{abs} \sim 278$, 230 nm, $\lambda_{flu} \sim 335$ nm), the absorption spectra of the sulpha drug molecules are blue shifted but the fluorescence spectra are red shifted in all solvents. In polar solvents, only a small spectral shift was observed in the absorption and emission maxima of the above sulpha drugs. This is because a tautomeric structure is present in sulpha drug molecules [17] (Scheme 2). For this reason, sulpha drug molecules are insoluble in the non-polar cyclohexane solvent. Though there is no discernible effect (not more than a few nm) of the solvent polarity on the absorption maxima, the spectral shifts observed in the absorption spectra of the above molecules in solvents are consistent with the characteristic behavior of the amino group [16–20].

The fluorescence spectra of the above molecules are displayed in Fig. 1. In all solvents, the above compounds have one broad structureless fluorescence maxima. The fluorescence spectra of the sulpha drug molecules are red shifted as the solvent polarity and proton donor/acceptor capacity increases. However, the emission maxima are almost the same in polar solvents; this is because the oxazole and thiazole groups are isoelectronic and their electronic spectra are expected to be similar. Hence, the spectral shifts of these molecules indicates that the emission maxima at 340 nm originate from the phenyl ring [20, 21]. Earlier, spectral studies of 2-arylbenzoxazoles in solvents [21] indicated that the aryl group acts as the main chromophore and its electronic transitions are perturbed by the oxazole moiety. The present experimental results in Table 1 also confirmed earlier results [19–21].

The electronic spectra of aryl amines have been studied extensively [16–20] and the red shift produced in the absorption spectra of the parent hydrocarbon is due to the resonance interaction of the lone pair of the amino nitrogen with the π-cloud of the parent hydrocarbon. This interaction increases if an electron withdrawing group is attached in the *para* position. Thus, the nature of the electron withdrawing group in the *para* position decides the percentage charge transfer character in the π–π^* transition as well as the value of the band maximum. The sulpha drug molecules also have a –SO_2– group as an electron withdrawing group in *para* position. The amino group conjugated with the electron withdrawing group (Scheme 2) can also inhibit more interaction between the solvents and these molecules. Further it is well known that the amino proton becomes a strong acid and the tertiary nitrogen and SO_2 groups become strong bases in S_1 their state. This is reflected in sulpha drug molecules, hence no large red shift is observed in protic solvents.

Table 1 Absorption and fluorescence spectral data (nm), and Stokes shift (cm^{-1}) observed for SFO, SMO, STO and SAM in different solvents

Solvents	SFO				SMO				STO				SAM			
	λ_{abs}	$\log_{10}\varepsilon$	λ_{flu}	Stokes shift	λ_{abs}	$\log_{10}\varepsilon$	λ_{flu}	Stokes shift	λ_{abs}	$\log_{10}\varepsilon$	λ_{flu}	Stokes shift	λ_{abs}	$\log_{10}\varepsilon$	λ_{flu}	Stokes shift
Cyclohexane	261.6	3.51	310	5968	260.6	3.75	316	7698	260.6	3.75	312	6322	260.0	3.40	320	7211
1,4-Dioxane	269.2	4.39	326	6472	267.0	4.13	334	7513	266.0	4.13	334	7654	260.0	3.45	336	8700
	235.0	3.96			232.0	3.61			232.0	3.61						
THF	270.8	4.28	330	6625	268.0	3.95	335	7563	268.4	3.95	335	7407	261.2	3.38	336	8523
	237.6	4.95			231.4	3.44			231.6	3.44						
Ethyl acetate	270.2	4.27	334	7070	268.0	3.90	336	7552	268.2	3.90	336	7524	261.4	3.38	336	8494
	235.6	4.84			230.6	3.48			230.2	3.48						
Acetonitrile	270.2	4.99	338	7424	269.2	3.98	337	7474	269.0	3.98	337	7500	261.6	3.53	336	8464
	237.6	4.51			212.2	3.79			213.2	3.79						
Chloroform	270.6	4.66	334	7015	269.4	4.33	335	7270	269.2	4.33	336	7385	261.0	3.38	336	8552
	231.2	4.10			232.2	3.75			231.0	3.75						
t-Butyl alcohol	271.6	4.71	338	7233	271.0	3.98	340	7489	271.0	3.98	341	7575	261.6	3.38	340	8815
	235.6	4.41			215.0	3.69			215.2	3.69						
2-Butanol	272.0	4.52	339	7266	272.0	4.18	340	7353	271.2	4.18	341	7548	261.4	3.35	340	8844
	235.6	4.46			211.4	3.83			213.4	3.83						
2-Propanol	272.0	4.51	339	7266	270.4	4.35	340	7570	271.2	4.35	341	7548	261.2	3.53	340	8874
	235.6	4.46			204.8	4.45										
Glycol	272.6	4.71	339	7186	271.8	4.05	340	7380	271.4	4.05	340	7434	261.4	3.52	340	8844
	235.6	4.41														

Table 1 (*Continued*)

Solvents	SFO				SMO				STO				SAM			
	λ_{abs}	$\log_{10}\varepsilon$	λ_{flu}	Stokes shift	λ_{abs}	$\log_{10}\varepsilon$	λ_{flu}	Stokes shift	λ_{abs}	$\log_{10}\varepsilon$	λ_{flu}	Stokes shift	λ_{abs}	$\log_{10}\varepsilon$	λ_{flu}	Stokes shift
Methanol	270.8 235.6	4.71 4.51	339	7430	269.8	4.19	340	7653	269.0	4.19	340	7763	261.2	3.52	340	8874
Water (pH = 6.5)	261.6	4.21	344	9157	261.6	3.75	342	8987	261.0	3.75	342	9075	258.0	3.21	341	9434
Excitation wavelength (nm)	270				270				270				270			
Correlation coefficient																
$E_T(30)$ versus $\Delta\overline{\nu}_{ss}$				0.8747				0.8864				0.8852				0.8726
BK versus $\Delta\overline{\nu}_{ss}$				0.6592				0.6416				0.6358				0.6276

λ_{abs}—absorption maximum in wavelength (nm)
λ_{flu}—emission maximum in wavelength (nm)
Stokes shift in cm^{-1}

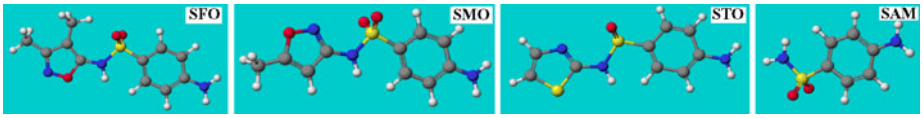

SFO: ΔH = -3.89668 kcal·mol^{-1} = -16.30370 kJ·mol^{-1}

H_1-H_6= 13.082	H_2-H_6= 12.710	H_6-H_{11}= 5.313	H_1-H_7= 12.493
H_2-H_7= 12.320	H_5-H_6= 6.190	H_1-H_8= 12.488	H_2-H_8= 12.315
H_5-H_7= 6.000	H_1-H_9= 10.505	H_2-H_9= 10.620	H_5-H_8= 5.998
H_1-H_{10}=10.505	H_2-H_{10}= 10.619	O_3-H_9= 4.295	H_1-H_{11}= 8.939
H_2-H_{11}= 9.142	O_3-H_{10}= 4.295	O_3-H_{11}= 4.138	H_1-N_2= 7.314
H_2-N_2= 7.005	H_6-S= 6.892	H_7-S= 6.156	H_8-S= 6.152

SMO: ΔH = 4.86508 kcal·mol^{-1} = 20.35551 kJ·mol^{-1}

H_1-H_9= 11.766	N_1-N_2= 6.617	H_7-S= 6.827	H_1-H_8= 12.372
N_1-S = 5.897	H_8-S= 6.827	H_1-H_7= 12.371	H_1-H_5= 6.548
H_9-S= 6.845	H_2-H_7= 12.836	H_2-H_5= 7.077	H_2-H_8= 12.837
H_5-H_7= 5.862	H_2-H_9= 12.429	H_5-H_8= 5.864	H_5-H_9= 5.360

STO: ΔH = 8.5254 kcal·mol^{-1}

H_1-H_8=12.481	H_2-H_8=11.854
H_3-H_5=5.071	H_1-S_2=11.345
N_1-N_2=6.923	N_1-N_3=9.252
N_1-S_2=6.201	H_9-S_1=6.332

SAM: ΔH = -45.93781 kcal·mol^{-1} = -192.20380 kJ·mol^{-1}

H_1-H_2= 1.706	H_1-O_1= 7.083	H_5-H_6= 1.637	H_1-O_2= 7.083
H_2-O_1= 6.867	H_1-H_5= 7.990	H_2-H_5= 8.290	H_2-O_2= 6.867
H_1-H_6= 6.604	N_1-N_2= 6.618	H_2-H_6= 7.130	N_1-S= 5.895

Scheme 1 CAChe-DFT structure—SFO, SMO, STO and SAM

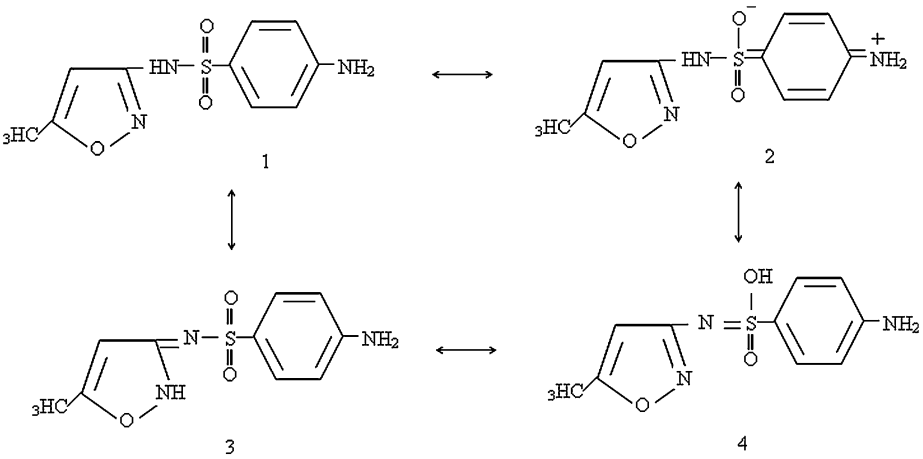

Scheme 2 Various resonance structures of SMO

In this study, the Stokes shifts of SFO, SMO, STO and SAM determined in different solvents of varying polarity have been correlated with the Biolet-Kawaski (BK) [22] and $E_T(30)$ [23] parameters. Table 1 gives list of solvents and their corresponding polarity para-

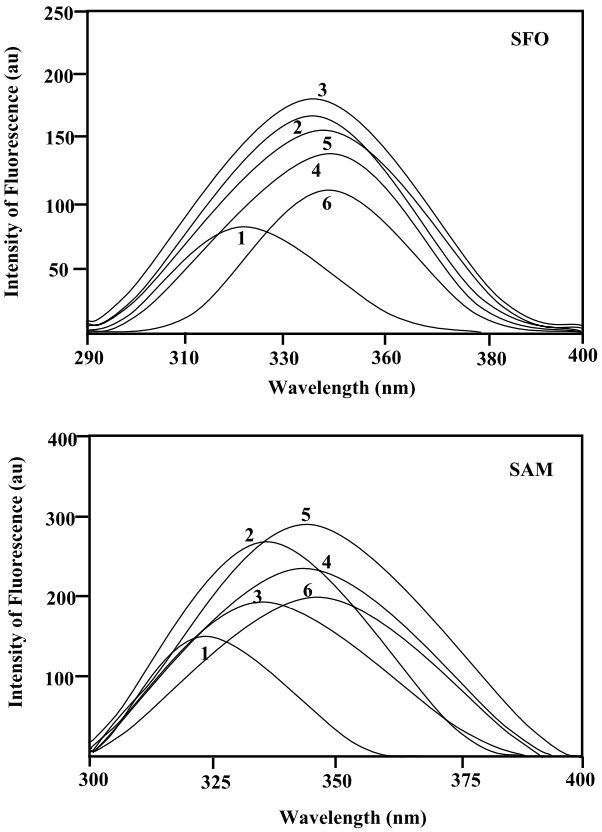

Fig. 1 Emission spectra of SFO and SAM in selected solvents at 303 K: *1*—cyclohexane, *2*—ethyl acetate, *3*—acetonitrile, *4*—2-propanol, *5*—methanol, *6*—water

meters and the Stokes shifts. Figure 2 in aprotic solvents indicates that nonspecific interactions are the key factors in shifting the fluorescence maxima to the red for these molecules. As it is evident from the slops of the plots, these interactions are large in the case of SAM and may be attributed to its increase of dipole moment of excitation. In the excited state, rigid molecules with limited internal degrees of freedom change the structure of the solvent cage by their dipole moment change. This process induces a large Stokes shifts in SAM in polar solvents. A good correlation of the Stokes shift with the $E_T(30)$ scale in Fig. 2 indicates the fact that the dielectronic solute-solvent interactions are responsible for the solvatochromic shifts in these molecules.

3.2 Effect of Hydrogen ion Concentration

The absorption and fluorescence spectra of the SFO, SMO, STO and SAM sulpha drug samples were studied in various acid-base concentrations in the H_0/pH/H_- range of −10 to 16.0 at room temperature (303 K). The spectral properties for their different prototropic species are listed in Table 2 and the spectra are shown in Figs. 3 and 4. The behavior of these molecules in the above range of acid-base regions are similar. With a decrease in pH from 7, the absorption and emission spectra of SAM are largely blue shifted (220 nm) at H_0 −0.80 with very weak absorption shoulder at 269, 266 nm, which indicates that a monocation is formed. No further change is noticed even at H_0 −10. When the pH is increased from 10, due to the

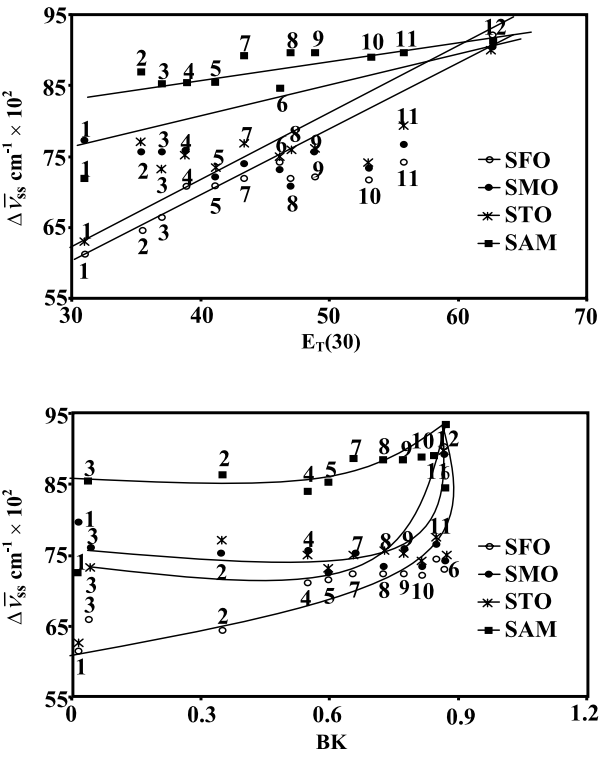

Fig. 2 Plot of Stokes shifts (cm^{-1}) of SFO, SMO, STO and SAM versus $E_T(30)$ and BK solvent parameters: *1*—cyclohexane, *2*—diethyl ether, *3*—1,4-dioxane, *4*—ethylacetate, *5*—dichloromethane, *6*—acetonitrile, *7*— *t*-butyl alcohol, *8*—2-butanol, *9*—2-propanol, *10*—ethanol, *11*—methanol, *12*—water

formation of a monoanion, the emission intensity of SAM is quenched at the same wavelength. In very high basicity (H_-16) a red shifted emission maximum is obtained indicating that a dianion is formed in the SAM molecule. None of the molecules show any change of absorption characteristics in the region pH ∼7 to 12, indicating that only neutral species are present in this pH range. Above pH ∼11, the fluorescence intensity decreases at the same emission wavelength suggesting that monoanions are formed. In general, the monoanions of many aromatic amino compounds are reported to be a non-fluorescent [24, 25]. A regular red shift is noticed in both absorption and fluorescence spectra in these pH ranges from 7.0 to 4.0, indicating the formation of a monocation. The monocation can be formed by protonation either at the ring nitrogen or in the $–NH_2$ group. The experimental results (Table 3) and those of Dogra et al. [24, 25] have clearly established that the first protonation takes place at the tertiary nitrogen atom. A similar behavior (i.e. red shift in absorption spectrum) has been observed during the first protonation of 2-(4′-aminophenyl) benzoxazoles [24, 25]. Further, when the hydrogen ion concentration is increased below pH ∼3, the absorption spectrum is largely blue shifted which indicates that protonation takes place in the $–NH_2$ group. It is a well known fact that protonation of an amino group gives blue shifted absorption maxima [27–30]. Furthermore, the absorption maxima of SMO, STO and SFO molecules resemble those of SAM, also indicating that the protonation takes place in the NH_2 group.

The dication absorption maxima of these molecules are largely blue shifted (220 nm) with very week shoulders that appear at 272 nm and 266 nm, which resemble those of the SAM monocation. The above absorption and fluorescence spectra of these molecules at H_0 −0.80, which resemble the monocation spectrum of SAM, can be assigned to the dication formed by protonation of the amino group. It is observed that the fluorescence intensity

Table 2 Various prototropic maxima (absorption and fluorescence) of SMO, SFO, STO and SAM in aqueous and β-CD medium

Species	SFO				SMO				STO				SAM			
	Aqueous medium		β-CD medium		Aqueous medium		β-CD medium		Aqueous medium		β-CD medium		Aqueous medium		β-CD medium	
	λ_{abs}	λ_{flu}	λ_{abs}	λ_{flu}	λ_{abs}	λ_{flu}	λ_{abs}	λ_{flu}	λ_{abs}	λ_{flu}	λ_{abs}	λ_{flu}	λ_{abs}	λ_{flu}	λ_{abs}	λ_{flu}
Dication	272ws	405	272ws	420	272ws	404	272ws	403	270	408	272	407				
	266ws	304	266ws	340	265ws	300	266ws	340	262	305	266	341				
	225		224		224		225		216		223					
Monocation	269	q	271	409wf	266	q	270	430wf	267	q	271	430	272ws	q		
	210			342s	210			342s	210		212	342	263ws			
													218			
Neutral	253	340	253	408	256	340ws	258	430	255	340	258	425	258	340	258	340
	205			340w	206			340w	206			340ws				
Dianion		415				418				420				430wf		

ws—weak shoulder
s—strong
q—quenching
wf—weakly fluorescent

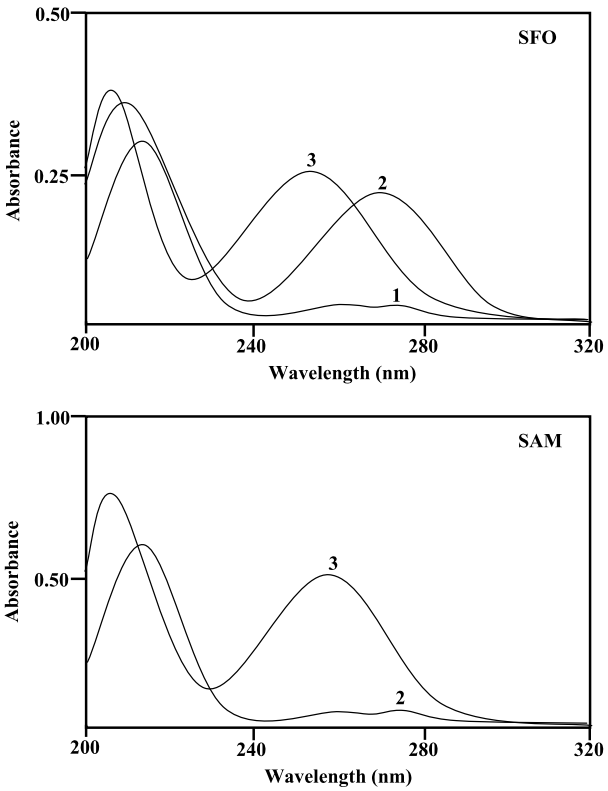

Fig. 3 Absorption spectra of different prototropic species of SFO and SAM at 303 K: concentration 4×10^{-5} Mol·L^{-1}. *1*—dication, *2*—monocation, *3*—neutral

of the monocation starts decreasing at pH ∼3 and a red shifted fluorescence band starts appearing only at H_0 −0.26. The decreased fluorescence intensity at the same emission wavelength could be due to either proton induced fluorescence quenching or formation of a non-fluorescence monocation.

3.3 Acidity Constants

The pK_a values for different prototropic reactions determined by using absorption data are listed in Table 3. Since the amino group in a sulpha drug molecule is resonance stabilized, the electron density at the amino group will be decreased (Scheme 2). Thus, a regular red shifted absorption maximum is observed in neutral to monocation species. The very low pK_a value for the dication-monocation equilibrium is due to the presence of a nearby positive charge on the amino group which reduces the electron density in the oxazole nitrogen atom. The pK_a^* values for different prototropic equilibria have been determined by fluorimetric titrations and the values clearly indicate that the amino group becomes a stronger acid upon excitation.

3.4 Interaction of Sulpha Drugs with β-CD

The absorption and emission spectra of SMO, SFO, STO and SAM were recorded in solution of β-CD at different concentrations (pH ∼ 7) and are shown in Table 4, Figs. 5 to 8. The absorption maxima of the above sulpha drug molecules are red shifted with a gradual increase in the molecular coefficient. The increase in the absorbance is due to the encap-

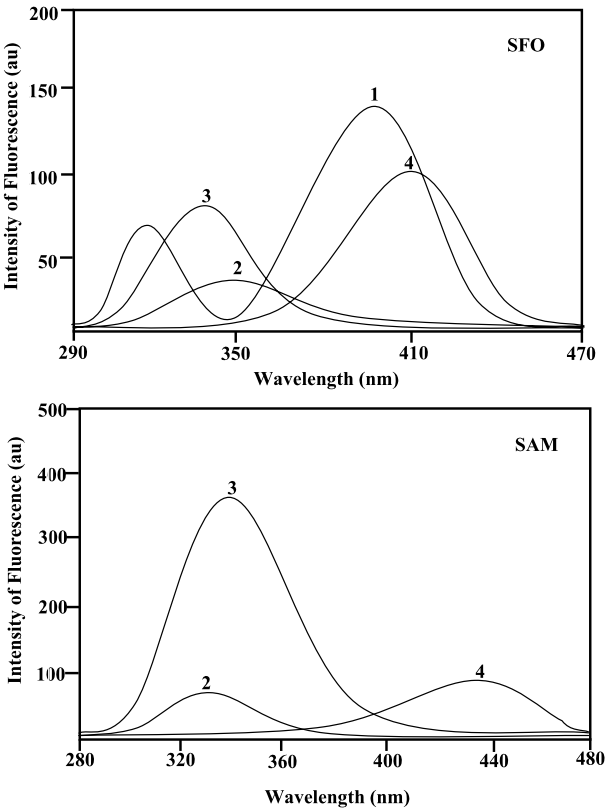

Fig. 4 Emission spectra of different prototropic species of SFO and SAM at 303 K: concentration 4×10^{-5} Mol·L^{-1}. *1*—dication, *2*—monocation, *3*—neutral, *4*—dianion

sulation of these molecules into the β-CD cavity and it is attributed to the detergent action of β-CD [31–34]. After preparing these drug-β-CD solutions, we also recorded the absorption spectra after 12 hrs. But no significant absorbance change is observed in these drug solutions, revealing that these drugs are encapsulated in the β-CD cavity and the inclusion complexes do not decompose upon storage. The above behavior may be attributed to the enhanced dissolution of the guest molecule through hydrophobic interaction between the guest and the non-polar cavity of the β-CD. These results indicate that sulpha drugs are entrapped in the β-CD to form inclusion complexes.

No clear isosbestic point is observed in the absorption spectra, but the changes that are observed in the absorbance are very small. In general, the existence of an isosbestic point in the absorption spectra is indicative of the formation of a well defined 1:1 complex [35–42]. These possibilities are proposed for this deviation: (i) more than one guest molecule can be accommodated within a single β-CD cavity, (ii) due to the space restriction of β-CD cavity, more than one type of complex with each having 1:1 stoichiometry may be formed, and (iii) the changes detected in the absorption spectra when β-CD is added to a sulpha drug solution containing methanol (1%) can also give rise to interaction between these components. Since, in these experiments the concentration of methanol is practically constant with respect to β-CD concentration, it may affect the isosbestic point. Further, in sulpha drug inclusion complexes, the detergent action of β-CD is so strong that no isosbestic point was observed in the absorption spectra. In the following discussions we propose two distinct complexes, one is the aniline part encapsulated and the other is the heterocyclic (i.e. five member ring) partly encapsulated into the β-CD cavity.

Table 3 pK_a and pK_a^* values of different prototropic equilibrium of SMO, SFO, STO and SAM in the S_0 and S_1 states

Equilibrium	SFO				SMO				STO				SAM			
	Aqueous medium		β-CD medium		Aqueous medium		β-CD medium		Aqueous medium		β-CD medium		Aqueous medium		β-CD medium	
	pK_a abs	pK_a^* FT	pK_a abs	pK_a^* FT	pK_a abs	pK_a^* FT	pK_a abs	pK_a^* FT	pK_a abs	pK_a^* FT	pK_a abs	pK_a^* FT	pK_a abs	pK_a^* FT	pK_a abs	pK_a^* FT
Dication Monocation	1.5	0.79	1.48	0.76	1.5	0.83	1.47	0.80	2.2	1.82	2.0	1.78				
Monocation Neutral	5.3	5.2	5.1	5.0	5.5	5.3	5.4	5.6	6.5	6.6	6.4	6.4	0.83	0.82	0.80	0.79
Neutral Monoanion	13.8	13.0			13.0	14.2			13.8	14.0	13.4	14.2	13.6	14.1		
Monoanion Dianion		16.2				15.6				15.5				15.6		

Table 4 Absorption and fluorescence maxima (nm) of SMO, SFO, STO and SAM at different concentrations of β-CD

Concentration of β-CD, Mol·L^{-1}	SFO			SMO			STO			SAM		
	λ_{abs}	$\log_{10}\varepsilon$	λ_{flu}	λ_{abs}	$\log_{10}\varepsilon$	λ_{flu}	λ_{abs}	$\log_{10}\varepsilon$	λ_{flu}	λ_{abs}	$\log_{10}\varepsilon$	λ_{flu}
Water	261.6	4.35	340	262.5	4.24	342	262.5	4.24	342	258	3.43	340
(without β-CD)	204.6	4.40		207.5	4.30		207.5	4.30				
0.001	268.0	4.31	336	268.0	4.27	341	268.0	4.27	342	258	3.51	340
	204.6	4.42	420	207.5	4.30	414	207.5	4.30	414			
0.002	268.4	4.39	337	268.5	4.28	341	268.5	4.28	341	258	3.52	340
	204.6	4.45	440	207.0	4.35	427	207.0	4.35	428			
0.004	268.8	4.40	339	268.0	4.34	341	268.0	4.34	341	258	3.60	340
	206.6	4.51	440	208.0	4.47	427	208.0	4.47	428			
0.006	268.6	4.40	339	268.5	4.35	341	268.5	4.35	341	258	3.64	340
	208.4	4.55	440	208.0	4.53	427	208.0	4.53	430			
0.008	268.6	4.43	339	269.0	4.38	341	269.0	4.38	341	258	3.68	340
	210.2	4.59	440	210.0	4.57	429	210.0	4.57	430			
0.010	269.6	4.47	340	269.5	4.43	341	269.5	4.43	341	258	3.74	340
	212.8	4.62	440	209.5	4.59	429	209.5	4.59	430			
Excitation wavelength (nm)	270			270			270			260		
Binding constant (L·Mol^{-1})	418		623	350		546	325		524	287		434
ΔG(-ve) kJ·Mol^{-1}	15.21		16.20	14.76		15.87	14.56		15.76	14.26		15.29

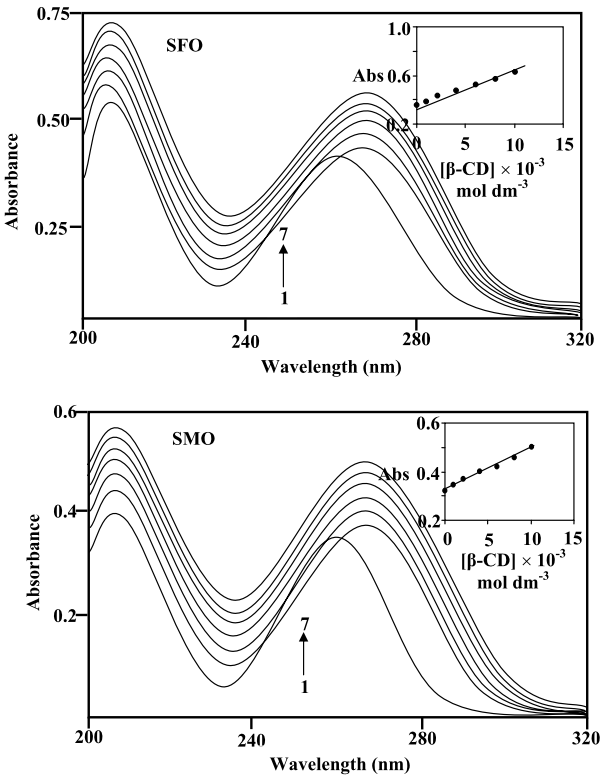

Fig. 5 Absorption spectra of SFO and SMO in different β-CD concentrations (Mol·L^{-1}): *1*—0, *2*—0.001, *3*—0.002, *4*—0.004, *5*—0.006, *6*—0.008, *7*—0.01. *Insert figure*: absorbance versus β-CD concentration

The binding constant for inclusion complex formation has been determined by the changes in the absorbance and fluorescence intensities with the β-CD concentrations. The binding constant (K) values were determined by using the Benesi-Hildebrand relation [43] and indicate that 1:1 complexes are formed between β-CD and these compounds. In all cases, k values 1:1 complexes formed between β-CD and these molecules were determined using the following equation:

$$\frac{1}{I - I_0} = \frac{1}{I' - I_0} + \frac{1}{K(I' - I_0)[\beta - \mathrm{CD}]_0} \tag{1}$$

where $[\beta\text{-CD}]_0$ represents the initial concentration of β-CD, I_0 and I are the absorbance and fluorescence intensities in the absence and presence of β-CD, respectively, and I' is the limiting intensity of absorbance and fluorescence. The 'K' values were obtained from the slope and intercept of the plots (Figs. 9 and 10). The Benesi-Hildebrand plot shows excellent linear regression supporting the formation of the 1:1 inclusion complex. The binding constant values are very small compared with other guest molecule/β-CD complexes such as dialkyl aminobenzonitrile and its derivatives [40–42]. This is probably because (i) sulpha drug molecules are partially included into the cavity, (ii) the oxazole/thiazole group may be included in the cavity, and (iii) these molecules are not tightly encapsulated in the β-CD cavity.

The change in standard Gibbs energy of this complex can be calculated from the:

$$\Delta G = -RT \ln K \tag{2}$$

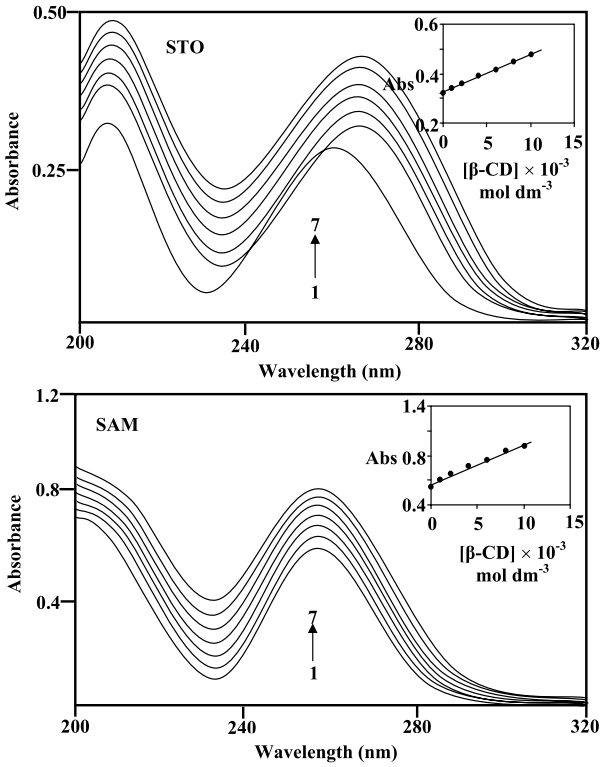

Fig. 6 Absorption spectra of STO and SAM in different β-CD concentrations (Mol·L^{-1}): *1*—0, *2*—0.001, *3*—0.002, *4*—0.004, *5*—0.006, *6*— 0.008, *7*—0.01. *Insert figure*: absorbance versus β-CD concentration

As can be seen from Table 4, the ΔG values are negative which suggests that the inclusion process proceeded spontaneously at 303 K. The negative values at the experimental temperature indicate that the inclusion process is an exothermic and enthalpy controlled process. The hydrophobic interaction between the internal wall of β-CD and guest molecules is an important factor for the stability of inclusion complexes. In sulpha drugs, it may be considered that the difference in the magnitude of the hydrophobic interaction is related to that of the contact area of the guest molecule with the internal wall of β-CD.

Several driving forces have been postulated for the inclusion complexation of CD with guest compounds: (1) Van der Waals forces; (2) hydrophobic interactions; (3) hydrogen bonding; (4) release of distortional energy of CD by binding of the guest; and (5) extrusion of 'high energy water' from the cavity of CD upon inclusion complex formation. Based on the thermodynamic parameter (ΔG) calculated for the inclusion of drugs, we conclude that the hydrogen bonding interaction, van der Waals interaction, and breaking of the water cluster around this polar drug compound mainly dominate the driving force for inclusion complex formation.

It is well known that the strength of interaction is also dependent on the size of the CD cavity and size of the substituent in the complex. This means that the interaction is more sensitive to the size of substituents and the CD in the complexation. The CDs are truncated, right-cylindrical, cone-shaped molecules, 7.8 Å in height with a central cavity. The diameters of the narrower and wider rim of the cavity for β-CD are 6.5 Å and 5.8 Å, respectively. It is well known that the van der Waals force including the dipole-induced dipole interactions are proportional to the distance between the drug and the wall of the CD

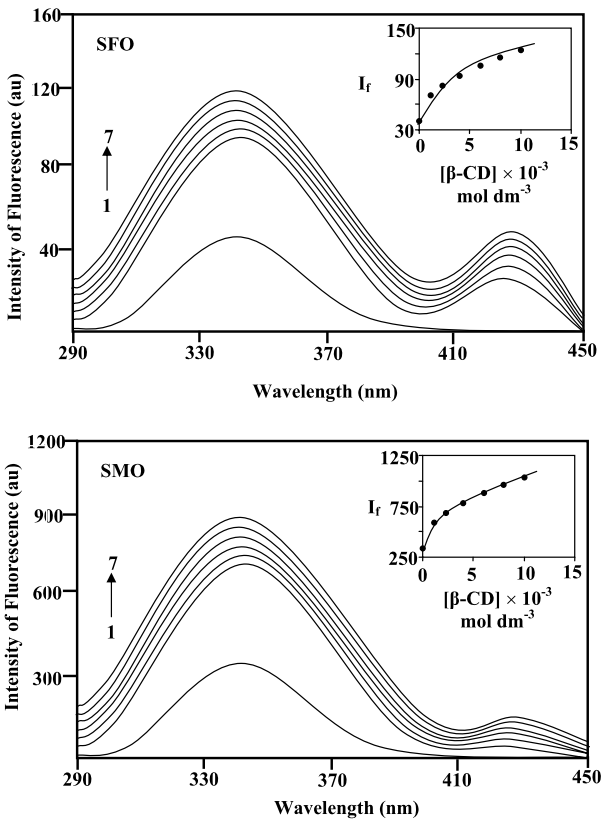

Fig. 7 Emission spectra of SFO and SMO in different β-CD concentrations (Mol·L^{-1}): *1*—0, *2*—0.001, *3*—0.002, *4*—0.004, *5*—0.006, *6*—0.008, *7*—0.01. *Insert figure*: fluorescence intensity versus β-CD concentration

cavity and to the polarizabilities of the two components. It is thus a short range interaction; therefore, the drug may be embedded deeper in β-CD. The phenyl moiety may achieve a maximum contact area with the internal surface of the cavity of the β-CD. Hence, the interaction of the phenyl ring with β-CD would play an important role.

In general, the inclusion of CDs with guest compounds is also affected by hydrophobic and electronic interactions. Since CDs have a permanent dipole, the primary hydroxyl end is positive and the secondary hydroxyl end is negative in the glucose units of CDs. The stability of binding by hydrophobic interaction is partly the result of the van der Waals force but is mainly due to the effects of entropy produced on the water molecules. In aqueous solution, a hydrophobic guest compound is restricted by the water shell formed by the hydrogen bonding network. It has a strong tendency to break down the water cluster and penetrate the non-polar cavity of CD. This process is exothermic due to an entropic gain. The association constants for the inclusion of β-CD with guest compounds were observed to be proportional to the substituent hydrophobic constant of the guest.

Figures 7 and 8 show the fluorescence spectra of the sulfa drugs SMO, SFO, STO and SAM in aqueous solution as a function of the β-CD concentration. Since no clear isosbestic point was observed in the absorption spectrum of a neutral molecule, the excitation wavelength is selected in such a manner that the absorbance changes are very small. In aqueous solution, a single fluorescence maximum was observed in the above sulpha drug molecules. Upon addition of β-CD, the emission band at 342 nm was gradually increased with an ap-

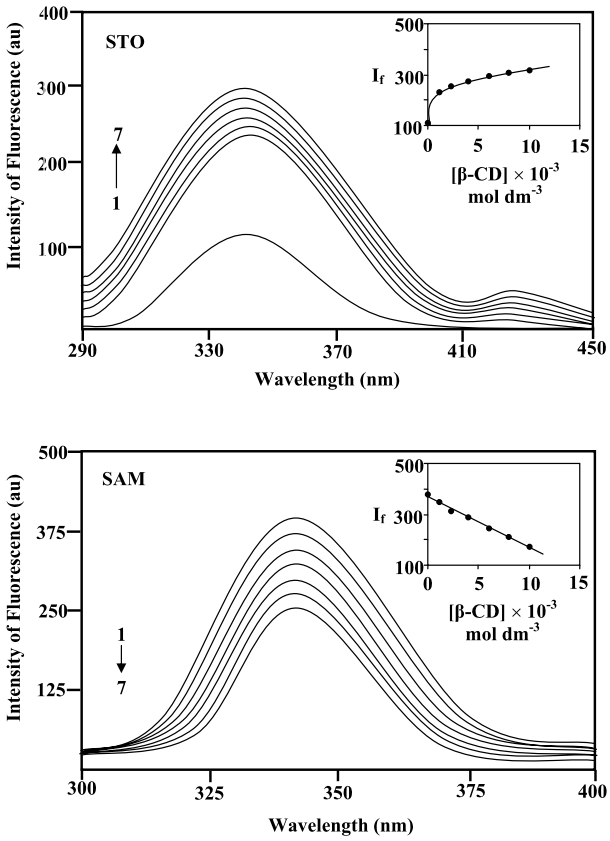

Fig. 8 Emission spectra of STO and SAM in different β-CD concentrations (Mol·L^{-1}): *1*—0, *2*—0.001, *3*—0.002, *4*—0.004, *5*—0.006, *6*—0.008, *7*—0.01. *Insert figure*: fluorescence intensity versus β-CD concentration

pearance of dual emission at 430 nm in SMO/SFO/STO molecules. In contrast in SAM, the emission intensity at 340 nm was gradually decreased without any dual emission.

The β-CD dependent emission spectra of sulpha drugs show that the shorter wavelength (SW) band is more sensitive in β-CD solutions, whereas the longer wavelength (LW) band shows a small enhancement with a regular bathochromic shift (Fig. 6). The LW intensity in β-CD medium is lower than the SW intensity. With addition of β-CD both LW and SW intensities are increased; however, the rate of enhancement of the SW emission is greater than that for the LW band. Further, with an increasing β-CD concentration, a regular red shift is observed in the LW band (420–430 nm) whereas no significant change is observed in the SW band (340 nm). This can be seen more clearly from observing Fig. 6, where the SW intensity in 0.010 Mol·L^{-1} β-CD solution is increased to 5 times that of the aqueous medium and the LW emission is enhanced by approximately 0.5 times. The enhancement of both bands of sulpha drug molecules in β-CD solutions may be explained as follows [44, 45]. The enhancement of the SW band in β-CD may be due to lowering of the solvent polarity at higher β-CD concentration [44, 45]. Inside the β-CD cavity sulpha drug molecule feels a much less polar environment and the main non-radiative path of the SW band (through intramolecular charge transfer (ICT) or twisted intramolecular charge transfer (TICT)) is restricted, which also causes an enhancement of the SW band. Further, the geometrical restriction of the cavity would restrict the free rotation of the heterocyclic ring

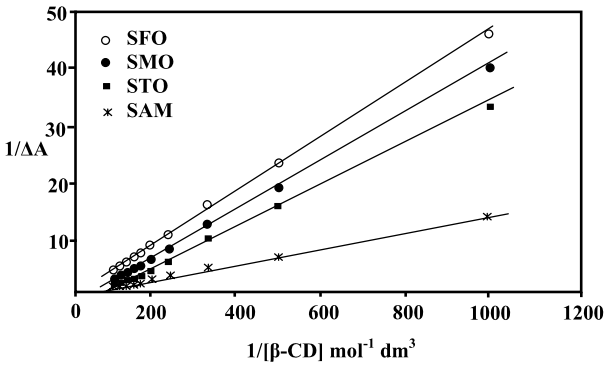

Fig. 9 Absorption spectra of the Benesi-Hildebrand plots for the complexation of SFO, SMO, STO and SAM with β-CD. Plot of $1/\Delta A$ versus $1/[\beta\text{-CD}]$

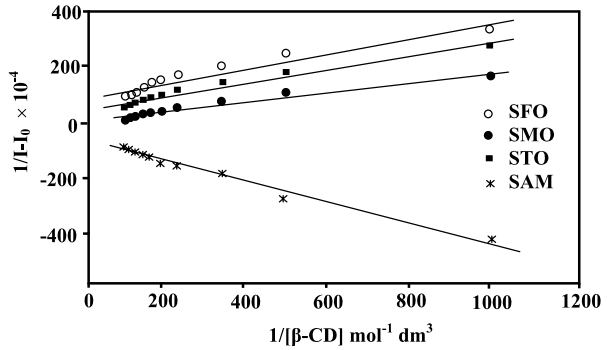

Fig. 10 Emission spectra of the Benesi-Hildebrand plots for the complexation of SFO, SMO, STO and SAM with β-CD. Plot of $1/I - I_0$ versus $1/[\beta\text{-CD}]$

or methyl group in the β-CD cavity and thus hinder the formation of an ICT state causing an enhancement of the normal SW band.

From the above findings it is clear that in β-CD solutions, the surrounding polarity of SO_2NH-group does not change very much as there is no hypsochromic shift of the most polar (ICT) state [46], but the relative intensity (I_{ICT}/I_{LE}) increases with the increase of β-CD concentration. This may be possible if the orientation of sulpha drugs is such that part of the aromatic ring goes inside the β-CD cavity (Scheme 3). This is because, if the amino group is present in the interior part of the β-CD cavity, a hypsochromic shift or ICT emission should not be present in the β-CD medium. We found that our earlier results, with aqueous β-CD solutions, hydrophobicity is the driving force for encapsulation of the molecule inside the cavity and naturally the hydrophobic part likes to go inside the deep core of the nonpolar cavity and the polar group will be projected in the hydrophilic part of the β-CD cavity [40–42].

The above results indicate that part of a SMO, SFO and STO molecule is entrapped in nonpolar β-CD cavity whereas SAM is completely included in the β-CD cavity to form an inclusion complex. Formation of the inclusion complex in SMO, SFO and STO with β-CD should result in dual emission. Since the size of SAM is smaller than the β-CD cavity size, this molecule may be completely included in the cavity; therefore, the emission intensity is decreased. However, the sizes of SMO, SFO and STO molecules are larger than the β-CD cavity size, and these molecules are partially included in the β-CD cavity (Schemes 1 and 3). Further, it is noteworthy that the LW emission intensity gradually increased along with the red shift upon increasing the β-CD concentrations. Thus, it can be suggested that the LW emission band is related to the formation of a β-CD inclusion complex. Such a spectral shift

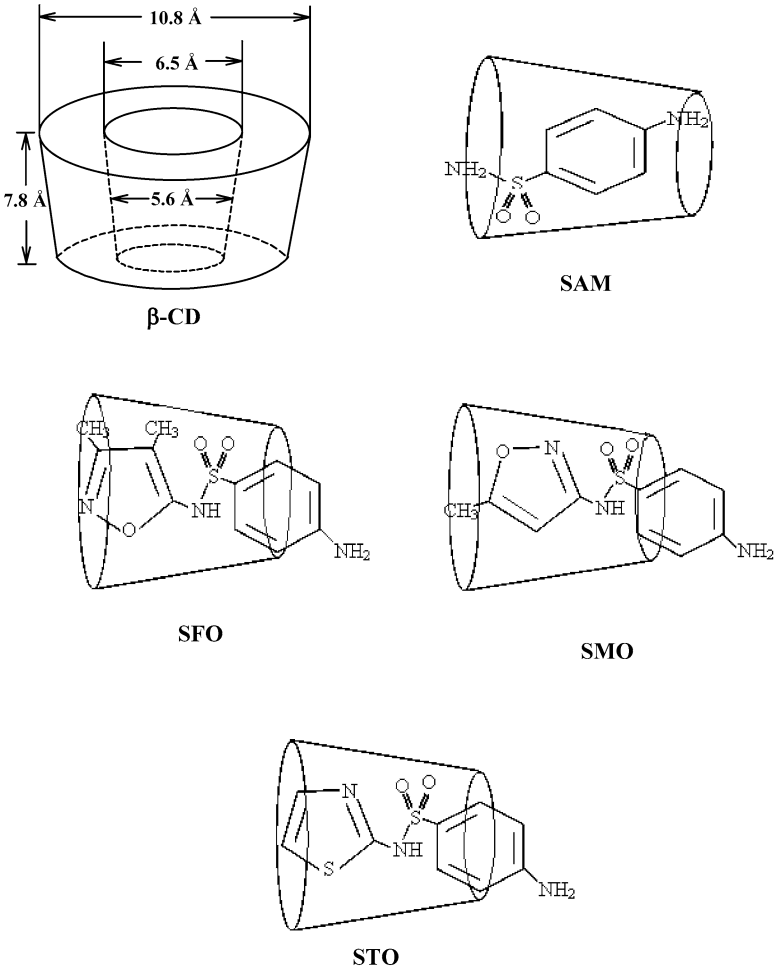

Scheme 3 The proposed inclusion complexes of SFO, SMO, STO and SAM

may correspond to an energy stabilization of the emitting state and is characteristic for the fluorescence of an ICT or TICT state. The LW emission from above sulfa drugs originate from the TICT state with twisting occurring at the amide S–N bond between the aniline moiety (electron donor) and the SO_2 moiety (electron acceptor). Further, Modiano et al. [47] reported whenever two aromatic rings are separated by groups like SO_2, CH_2, CO, NH etc. they form a TICT state. Thus it can be speculated that the enhanced 430 nm emission in the above sulfa drugs should originate from the TICT state. The TICT emission is observed in β-CD suggesting that the inclusion process plays a major role in the TICT emission. Supporting this implication, the excitation spectra for the 440 nm emission is similar to that of the 340 nm emission.

3.5 Prototropic Reactions in β-CD Medium

To know the effect of β-CD on the prototropic equilibrium between neutral, monocation and dication, pH dependent changes in the absorption and emission spectra of the sulpha

drug molecules in aqueous solution containing β-CD have been recorded and are shown in Table 2. The absorption and emission maxima of these molecules have been studied in 6×10^{-3} Mol·L^{-1} β-CD solutions in the pH range from 0.1 to 11. On comparison with aqueous medium, in β-CD solutions the absorption and emission maxima of these neutral drug molecules are red shifted (Table 2). The ground and excited state pK_a (pK_a^*) values of these molecules in β-CD medium are slightly lower than those in aqueous medium (Table 3). However, a red shift is observed in the β-CD solutions compared to the aqueous solutions, suggesting the sulpha drug molecules are encapsulated in the β-CD.

3.6 Possible Inclusion Complex

Considering the above discussions, the possible inclusion mechanism is proposed as follows. Naturally, two different types of inclusion complex formation between SMO, SFO and STO molecules with β-CD are possible: (i) the aniline group is captured in the β-CD cavity and (ii) the oxazole group is captured in the β-CD cavity. Let us consider the type I arrangement; if the aniline part is entrapped into the β-CD cavity, like SAM, the fluorescence intensities should decrease at higher β-CD concentrations. In this case, SMO, SFO and STO molecules should not show dual emission in β-CD medium. Further, if the amino group is entrapped into the β-CD cavity, the dication maxima [40–42] (i.e. protonation of amino group) should be blue shifted in β-CD compared to aqueous medium. But the results in Table 3 shows no significant spectral shifts either in the β-CD and aqueous medium; i.e., the dication maxima follow the same trend both in aqueous and β-CD medium.

For type II encapsulation, the oxazole group may be included in the β-CD cavity. If this type of complex is formed, the neutral maxima of the sulpha drugs (protonation of tertiary nitrogen atom) should be red shifted in β-CD compared with aqueous medium. The red shift observed in pH∼7 β-CD solution indicates that the tertiary nitrogen atom interacts with β-CD hydroxyl groups, because it is well known that CDs are good hydrogen donors [31–34]. Furthermore, the results observed for sulpha drugs are similar to amino benzoic acids [27–29] and 2,6-diaminopyridine [48]. The tendencies of these shifts in λ_{abs} and λ_{flu} of these molecules are attributable to the inclusion into the β-CD cavity, and are explained in Scheme 3. This is because of the formation of inclusion complex, i.e. in the inclusion complexes, pK_a (pK_a^*) values are known to change depending upon relative the affinity of the guest and host [40–42].

Further, in Type II complexes, the β-CD cavity will impose a restriction on the free rotation of the CH_3 group or oxazole and thiazole groups in its excited state. For this type, the TICT emission should increase in β-CD solutions. The question may arise why TICT emission is not observed in SAM. This is because even this complex formation does not affect the free rotation of $–SO_2–NH_2$ group because the size of SAM is smaller than the β-CD cavity size. Further, another question may arise why SMO, SFO and STO do not exhibit the TICT emission in polar and nonpolar solvents because of a weak dipole–dipole interaction between R–SO_2–NH-group with solvent and fast back-charge transfer. These features support the idea that the TICT state in β-CD is stabilized through complex formation between SMO/SFO/STO with β-CD. This confirms that the environments around the anilino group in β-CD medium are the same as in the bulk aqueous medium. These features indicate that in Scheme 3, type-II complex is favored more than type-I.

This is further supported by semi-empirical quantum mechanical calculations: the ground state geometry of the sulpha drugs were optimized by using the DFT method (CaChe 7.5 program). The internal diameter of β-CD is approximately 6.5 Å and its height is 7.8 Å. The vertical distance between the sulpha drug molecules are higher than the β-CD cavity size

and the horizontal distance is smaller than the β-CD cavity size (Scheme 1). Considering the shape and dimensions of β-CD and sulpha drugs, the only way sulpha drugs can enter into the β-CD is lengthwise. Under this situation, it is impossible for the sulpha drugs to be encapsulated completely in one β-CD molecule. Taking into account the dimensions of the sulpha drugs and β-CD, the complex can be located as shown in Scheme 3.

4 Solid Inclusion Complex Studies

4.1 Microscopic Morphological Observation

First we recorded the powdered form of the above sulfa drugs and β-CD by scanning electron microscope and then we also observed the powdered form of the inclusion complex (Fig. 11). These pictures clearly elucidate the difference of all sulfa drugs and their inclusion complex. As seen from the SEM figures, (i) β-CD is present in a platted form, and (ii) sulfa drugs are present in different forms from their inclusion complexes. Modification of these structures can be assumed as a proof of the formation of a new inclusion complex. The different structure of pure sulfa drugs and their inclusion complex again support the presence of a solid inclusion complex.

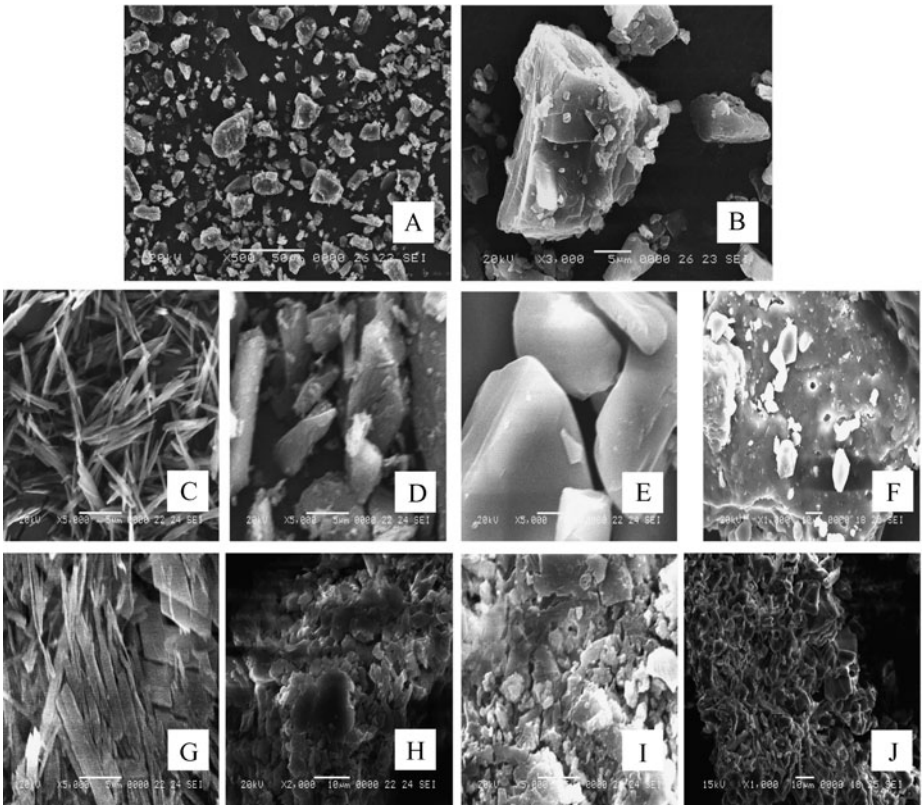

Fig. 11 Scanning electron microscope photographs (Pt coated) of (A, B) β-CD, (C) SFO, (D) SMO, (E) STO, (F) SAM, (G) SFO–β-CD complex, (H) SMO–β-CD complex, (I) STO–β-CD complex, (J) SAM–β-CD complex

4.2 FTIR Spectra of Sulfa Drugs

(i) SAM: The FTIR spectra of SMO, SFO, STO and SAM and the solid inclusion complex were also studied. The sharp amino stretching at 3477 cm^{-1} and amide NH stretching at 3373 cm^{-1} shifts to 3473 cm^{-1}, while the NH_2 deformation at 1629 cm^{-1} shifts to 1639 cm^{-1} in the inclusion complex. In addition, the C–N stretching at 1312 cm^{-1} moves to 1335 cm^{-1} and CH bending at 899–622 cm^{-1} moves to 858–706 cm^{-1}. The CH stretch at 3065 cm^{-1}, however, is absent in the complex, as well the C=C stretching at 3098 cm^{-1} is not present in the inclusion complex. The aromatic ring stretching at 1593 cm^{-1} does not appeare in the inclusion complex. The S=O stretch 1094 cm^{-1} moves in the inclusion complex to 1080 cm^{-1} and the SO_2NH_2 symmetric stretch 1148 cm^{-1} and anti-symmetric stretch 1312 cm^{-1} are moved in the inclusion complex to 1156 cm^{-1} and 1335 cm^{-1}, respectively. The overtone frequencies around 2600 to 2000 cm^{-1} are lost in the inclusion complex. The above finding indicates that a SAM molecule is included in the β-CD cavity and form an inclusion complex.

(ii) SMO: The amino sharp stretch at 3378 cm^{-1} and the amido sharp stretch at 3467 cm^{-1} changed in the inclusion complex to a broad peak that appears at 3378 cm^{-1}. The SO_2 anti-symmetric stretch at 1366 cm^{-1} is shifted in the inclusion complex to 1368 cm^{-1} and the symmetric stretch 1144 cm^{-1} is moved to 1157 cm^{-1}. Aromatic CH stretch at 3144 cm^{-1} does not appear in the inclusion complex. The CH bending peak at 885 to 684 cm^{-1} moves in the inclusion complex to 860–707 cm^{-1}. The aromatic C=C stretch at 3239 cm^{-1} is not present in the inclusion complex. The aromatic ring stretching at 1621 cm^{-1} moves in the inclusion complex to 1638 cm^{-1}. The CH stretching in C–CH_3 group at 2930 cm^{-1} is also not present in this complex. The CH_3 anti-symmetric stretch at 1472 cm^{-1} moves in the inclusion complex to 1413 cm^{-1}. The CN stretch at 1266 cm^{-1} is moved in the inclusion complex to 1244 cm^{-1}. The SO_2 stretch at 1026 cm^{-1} moves to 1029 cm^{-1}. Further the absorption intensity ratio between the drugs and their inclusion complexes are variable. The above results confirm that this molecule is encapsulated in the CD cavity.

(iii) SFO: The sharp NH stretch at 3381 cm^{-1} and amido stretch at 3485 cm^{-1} become broad in the inclusion complex. The CH stretch at 3095 cm^{-1} is lost and the bending at 876–688 cm^{-1} moves in the inclusion complex to 862–707 cm^{-1}. The C=C stretch at 3003 cm^{-1} does not appear in the inclusion complex. The C=C bending at 1596 cm^{-1} shifts in the inclusion complex to 1596 cm^{-1}. The methyl stretching at 1345 cm^{-1}, 1438 cm^{-1} is not shifted but the intensities are greatly reduced in this complex. The SO_2 stretching at 1345 cm^{-1} appears at the same peak. The C–NH_2 stretch at 1301 cm^{-1} is moved in the inclusion complex to 1345 cm^{-1}, 1330 cm^{-1}. The aromatic ring stretching at 1323 cm^{-1} is moved in the inclusion complex to 1330 cm^{-1}. Further, the aromatic overtone frequencies at 2000–1800 cm^{-1} are lost in the inclusion complex. The above results confirm this molecule is encapsulated in the CD cavity.

4.3 ^{1}H NMR Spectral Studies

Proton nuclear magnetic resonance (^{1}H NMR) spectroscopy has proved to be a powerful tool in the study of inclusion complexes [49, 50]. ^{1}H NMR spectroscopy provides an effective means of assessing the dynamic interaction site of β-CD with that of the guest molecules. The basis of information gained from NMR spectroscopy is located in this shifts, loss of resolution and broadening of signals observed for the host and guest protons [49, 50].

The resonance assignments of the protons of β-CD are well established [49, 50] and consist of six types of protons. The chemical shift of β-CD protons reported by different

authors [49, 50] are very close to those reported in this work. The H-3 and H-5 protons are located in the interior of the β-CD cavity and it is, therefore, likely that the interaction of the host with the β-CD inside the cavity will affect the chemical shifts of the H-3 and H-5 protons. A minor shift is observed for the resonance of H-1, H-2 and H-4 located on the exterior of β-CD.

The addition of sulpha drugs into the β-CD results in a downfield chemical shift for the sulpha drug protons in DMSO are given below (Scheme 3): SAM (inclusion complex) values in ppm: $NH_2 \sim 5.76$ (5.78), $SO_2NH_2 \sim 6.86$ (6.92), $^2H/^6H \sim 7.45$ (7.50), $^3H/^5H \sim 6.59$ (6.64); SMO (inclusion complex) values in ppm: $NH_2 \sim 6.10$ (6.12), $SO_2NH \sim 10.95$ (11.02), $^2H/^6H \sim 7.485$ (7.498), $^3H/^5H \sim 6.598$ (6.602), $CH_3 \sim 2.290$ (2.297), $^2H' \sim 6.107$ (6.111); SFO (inclusion complex) values in ppm: $NH_2 \sim 6.15$ (6.17), $SO_2NH \sim 11.25$ (11.30), $^2H/^6H \sim 7.480$ (7.484), $^3H/^5H \sim 6.604$ (6.607), $^{3'}CH_3 \sim 2.295$ (2.299), $^{4'}CH_3 \sim 2.303$ (2.307); STO (inclusion complex) values in ppm: $NH_2 \sim 5.90$ (5.92), $SO_2NH \sim 12.41$ (12.47), $^2H/^6H \sim 7.456$ (7.462), $^3H/^5H \sim 6.579$ (6.583), $^2H' \sim 7.196$ (7.201), $^3H' \sim 6.746$ (6.750). As can be seen from the above values, the chemical shifts data for the inclusion complex are different from the free compound. A small downfield shift on sulpha drugs was observed, suggesting that the studied molecules are encapsulated into the β-CD cavities.

5 Conclusion

From the above studies we find out the following points: Solvent studies reveal that the position of the substituent (oxazole or thiazole group) in the SAM molecule (R–SO_2–NH–) group is not the key factor to change the absorption and emission behavior of these molecules. In sulpha drugs, a single fluorescence band was observed in aqueous solution and dual emission appears in β-CD solution, indicating that the heterocyclic ring is encapsulated into the β-CD cavity. Formation of the inclusion complex in SMO, SFO and STO should result in dual emission, which is due to the presence of TICT. β-CD studies indicate (i) sulpha drugs form 1:1 inclusion complexes with β-CD, and (ii) the red shift in the β-CD medium confirms heterocyclic ring encapsulated in the β-CD cavity and the aniline ring is present on the outside of the β-CD cavity.

Acknowledgements This work was supported by the Department of Science and Technology, New Delhi (Fast Track Proposal Young Scientist Scheme No. SR/FTP/CS-14/2005) and University Grants Commission, New Delhi (Project No. F-31-98/2005 (SR). One of the authors A. Antony Muthu Prabhu is thankful to CSIR, New Delhi for the award of Senior Research Fellowship (SRF).

References

1. Scypinski, S., Love, J.L.C.: Cyclodextrin-induced room-temperature phosphorescence of nitrogen heterocycles and bridged biphenyls. Anal. Chem. **56**, 331–336 (1984)
2. Muñoz de la Peña, A., Durán Merás, I., Salinas, F., Warner, I.M., Ndou, T.T.: Cyclodextrin-induced fluid solution room temperature phosphorescence from acenaphthene in the presence of 2-bromoethanol. Anal. Chim. Acta **255**, 351–336 (1991)
3. Szente, L., Szejtli, J.: Non-chromatographic analytical uses of cyclodextrins. Analyst **123**, 735–741 (1998)
4. Okamoto, H., Uetake, A., Tamaya, R., Nakajima, T., Sagara, K., Ito, Y.: Simultaneous determination of eleven ingredients in ophthalmic solutions by cyclodextrin-modified micellar electrokinetic chromatography with tetrabutylammonium salt. J. Chromatogr. A **888**, 299–308 (2000)
5. Mora Diez, N., Muñoz de la Peña, A., Mahedero Garcia, M.C., Bohoyo Gil, D., Canada-Canada, F.: Fluorimetric determination of sulphaguanidine and sulphamethoxazole by host-guest complexation in β-cyclodextrin and partial least squares calibration. J. Fluoresc. **17**, 309–318 (2007)

6. Marek, J., Marek, J.: Farmakoterapie vnitrnich nemoci (Pharmacotherapy of Internal Diseases). Grada Publishing, Prague (1998), pp. 159
7. Msagati, T.A.M., Nindi, M.M.: Multiresidue determination of sulfonamides in a variety of biological matrices by supported liquid membrane with high pressure liquid chromatography-electrospray mass spectrometry detection. Talanta **64**, 87–100 (2004)
8. Bridges, J.W., Gifford, L.A., Hayes, W.P., Miller, J.N., Thorburn Burns, D.: Luminescence properties of sulfonamide drugs. Anal. Chem. **46**, 1010–1017 (1974)
9. Sterling, J.M., Haney, W.G.: Spectrophotofluorometric analysis of procainamide and sulfadiazine in presence of primary aliphatic amines based on reaction with fluorescamine. J. Pharm. Sci. **63**, 1448–1450 (1974)
10. Arthur, J., de Silva, F., Strojny, N.: Spectrofluorometric determination of pharmaceuticals containing aromatic or aliphatic primary amino groups as their fluorescamine (Fluram) derivatives. Anal. Chem. **47**, 714–718 (1975)
11. Stewart, J.T., RE, Wilkin: Determination of sulfonamides and local anesthetics with 9-chloroacridine by quenching fluorometry. J. Pharm. Sci. **61**, 432–433 (1972)
12. Pang, G.F., Cao, Y.Z., Fan, C.L., Zhang, J.J., Li, X.M., Li, Z.Y., Jia, G.Q.: Liquid chromatography fluorescence detection for simultaneous analysis of sulfonamide residues in honey. Anal. Bioanal. Chem. **376**, 534–541 (2003)
13. Maudens, E., Zhang, G.-F., Lambert, W.E.: Quantitative analysis of twelve sulfonamides in honey after acidic hydrolysis by high-performance liquid chromatography with post-column derivatization and fluorescence detection. J. Chromatogr. **1047**, 85–92 (2004)
14. Jorgenson, M.J., Hartter, D.R.: A critical re-evaluation of the Hammett acidity function at moderate and high acid concentrations of sulfuric acid. New H_0 values based solely on a set of primary aniline indicators. J. Am. Chem. Soc. **85**, 878–883 (1963)
15. Yagil, G.: The effect of ionic hydration on equilibria and rates in concentrated electrolyte solutions. IV. The H_ scale in concentrated hydroxide solutions. J. Phys. Chem. **71**, 1045–1052 (1967)
16. Rajendiran, N., Swaminathan, M.: Luminescence characteristics of 4,4′-diaminodiphenyl methane in different solvents and at various pH. Spectrochim. Acta A **52**, 1785–1792 (1996)
17. Rajendran, N., Swaminathan, M.: Photoluminescence of 4,4′-diaminodiphenyl. Bull. Chem. Soc. Jpn. **68**, 2797–2802 (1995)
18. Rajendiran, N., Swaminathan, M.: Unusual spectral shifts of bis(4-amino phenyl) ether. Bull. Chem. Soc. Jpn. **69**, 2447–2452 (1996)
19. Dey, J.K., Dogra, S.K.: Solvatochromism and prototropism in 2-(aminophenyl) benzothiazoles. Bull. Chem. Soc. Jpn. **64**, 3142–3152 (1991)
20. Mishra, A.K., Dogra, S.K.: Effect of solvents and pH on the spectral behavior of 2-(*p*-aminophenyl)benzimidazole. Bull. Chem. Soc. Jpn. **58**, 3587–3592 (1985)
21. Dey, J.K., Dogra, S.K.: Spectral characteristics of three different isomeric 2-(amino phenyl) benzoxazoles: effect of solvents and acid concentrations. Chem. Phys. **143**, 97–107 (1990)
22. Bilot, L., Kawasaki, A.: Zur theory des einflusses von loesungsmitteln auf die elektronenspektren der molekuele. Z. Naturforsch. A **17**, 621–630 (1962)
23. Reichardt, C.: Empirical parameters of solvent polarity as linear free-energy relationships. Angew. Chem. Int. Ed. English **18**, 98–110 (1979)
24. Mishra, A.K., Dogra, S.K.: Absorption and fluorescence spectra of 2-amino benzimidazole: effect of different solvents and pH on spectral behavior. Indian J. Chem. A **24**, 815–819 (1985)
25. Swaminathan, M., Dogra, S.K.: Solvent and Ph dependence of absorption and fluorescence spectra of 5-aminoindazole: biprotonic phototautomerism of singly protonated species. J. Am. Chem. Soc. **105**, 6223–6228 (1983)
26. Stalin, T., Rajendiran, N.: Intra molecular charge transfer effects on 3-aminobenzoic acid. Chem. Phys. **322**, 311–322 (2006)
27. Stalin, T., Rajendiran, N.: Intramolecular charge transfer effect associated with hydrogen bonding on 2-aminobenzoic acid. J. Photochem. Photobiol. A, Chem. **182**, 137–150 (2006)
28. Stalin, T., Rajendiran, N.: Solvatochromism, prototropism and complexation of para-aminobenzoic acid. J. Incl. Phenom. Macrocycl. Chem. **55**, 21–29 (2006)
29. Muthu Prabhu, A., Rajendiran, N.: Unusual spectral shifts on fast violet-B and benzanilide: effect of solvents, pH and β-cyclodextrin. Spectrochim. Acta A **74**, 484–497 (2009)
30. Muthu Prabhu, A., Rajendiran, N.: Azo-ammonium tautomerism and assembly behavior of inclusion complexes of β-cyclodextrin with 4-amino, 2′,3-dimethyl azobenzene and 4-amino azobenzene. Ind. J. Chem. **49A**, 407–417 (2010)
31. Kim, Y., Yoon, M., Kim, D.: Excited-state intramolecular proton transfer coupled-charge transfer of *p*-*N*,*N*-dimethylaminosalicylic acid in aqueous β-cyclodextrin solutions. J. Photochem. Photobiol. A **138**, 167–175 (2001)

32. Kim, T.H., Cho, D.W., Yoon, M., Kim, D.: Observation of hydrogen-bonding effects on twisted intramolecular charge transfer of *p*-(*N*,*N*-diethylamino)benzoic acid in aqueous cyclodextrin solutions. J. Phys. Chem. **100**, 15670–15676 (1996)
33. Jiang, Y.B.: Effect of cyclodextrin inclusion complex formation on the twisted intramolecular charge transfer (TICT) of the included compound: the *p*-dimethyl aminobenzoic acid-β-cyclodextrin system. J. Photochem. Photobiol. A, Chem. **88**, 109–116 (1995)
34. Jiang, Y.B.: Fluorescence spectroscopic investigation of the effect of α-cyclodextrin on the twisted intramolecular charge transfer of *p*-dimethylaminobenzoic acid in aqueous media. Appl. Spectrosc. **48**, 1169–1173 (1994)
35. Stalin, T., Rajendiran, N.: Photophysical behavior of 4-hydroxy-3,5-dimethoxy benzoic acid in different solvents, pH and β-cyclodextrin. J. Photochem. Photobiol. A, Chem. **177**, 144–155 (2006)
36. Stalin, T., Rajendiran, N.: Photophysical properties of 4-hydroxy-3-methoxy benzoic acid. J. Mol. Struct. **794**, 35–45 (2006)
37. Rajendiran, N., Balasubramanian, T.: Intramolecular charge transfer effects on 4-hydroxy-3-methoxy benzaldehyde. Spectrochim. Acta A **69**, 822–829 (2008)
38. Rajendiran, N., Balasubramanian, T.: Dual luminescence of syringaldazine. Spectrochim. Acta A **68**, 894–904 (2007)
39. Agbaria, RA, Uzar, B., Gill, D.: Fluorescence of 1,6-naphthalenediol with cyclodextrins. J. Phys. Chem. **93**, 3855–3859 (1989)
40. Sandra, S., Dogra, S.K.: Spectral characteristics of 2-(2′-aminophenyl)benzimidazole in β-cyclodextrin. J. Photochem. Photobiol. A, Chem. **101**, 221–227 (1996)
41. Krishnamoorthy, G., Dogra, S.K.: Dual fluorescence of 2-(4′-*N*,*N*-dimethyl amino phenyl)benzimidazole: effect of β-cyclodextrin and pH. J. Photochem. Photobiol. A, Chem. **123**, 109–119 (1999)
42. Das, S.: Inclusion complexation of 2-(4′*N*,*N*-dimethyl aminophenyl)-*1H*-naphth[*2,3-d*]imidazole by β-cyclodextrin: effect on the twisted intramolecular charge transfer emission. Chem. Phys. Lett. **361**, 21–28 (2002)
43. Benesi, A., Hildebrand, J.H.: A spectrophotometric investigation of the interaction of iodine with aromatic hydrocarbons. J. Am. Chem. Soc. **71**, 2703–2707 (1949)
44. Bhattacharya, K., Chowdhury, M.: Environmental and magnetic field effects on exciplex and twisted charge transfer emission. Chem. Rev. **93**, 507–535 (1993)
45. Panja, S., Bangal, P.R., Chakravorty, S.: Modulation of photophysics due to orientational selectivity of 4-*N*,*N*-dimethylaminocinnamladehyde β-cyclodextrin inclusion complex in different solvents. Chem. Phys. Lett. **329**, 377–385 (2000)
46. Testa, A.C.: Evidence for a hydrogen bonded dimer as a fluorescence quenching channel in 4,5-diphenylimidazole. J. Luminesci. **50**, 243–248 (1991)
47. Modiano, S.H., Dresner, J., Lim, B.C.: Intramolecular photoassociation and photoinduced charge transfer in bridged diaryl compounds. 1. Photoassociation in the lowest triplet state of 2,2′-dinaphthylmethane and 2,2′-dinaphthyl ether. J. Phys. Chem. **95**, 9144–9151 (1991)
48. Muthu Prabhu, A.A., Siva, S., Sankaranarayanan, R.K., Rajendiran, N.: Intra molecular proton transfer effects on 2,6-diaminopyridine. J. Fluoresc. **20**, 43–54 (2010)
49. Lehman, J., Klienpeter, E.: ^{1}H NMR spectroscopy as a probe of intermolecular interactions in β-cyclodextrin inclusion compounds. J. Incl. Phenom. **10**, 233–239 (1991)
50. Rath, M.C., Palit, D.K., Mukherjee, T.: Effects of organised media on the excited-state proton transfer in 2-(2′-pyridyl)benzimidazole. J. Chem. Soc. Faraday Trans. **94**, 1189–1196 (1998)